Short Article

Cell Metabolism

α-Ketoglutarate Accelerates the Initial Differentiation of Primed Human Pluripotent Stem Cells

Graphical Abstract

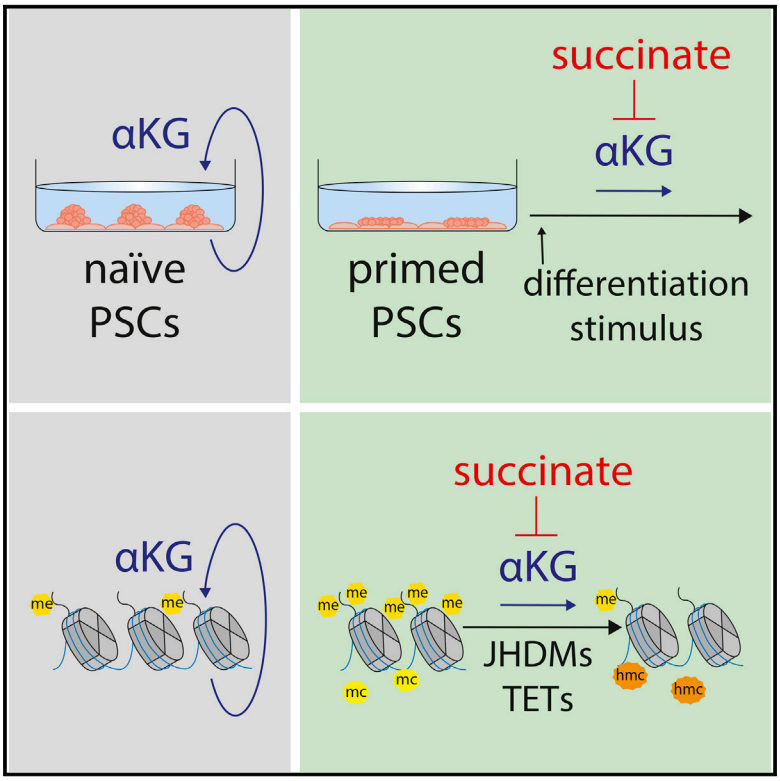

Highlights

- hPSCs produce TCA cycle metabolites despite low OXPHOS
- α-ketoglutarate (αKG) promotes early differentiation of hPSCs
- Accumulation of succinate or depletion of αKG delays differentiation of hPSCs
- αKG/succinate alters histone methylation corresponding to differentiation kinetics

Authors

Tara TeSlaa, Andrea C. Chaikovsky, Inna Lipchina, ..., Thomas G. Graeber, Daniel Braas, Michael A. Teitell

Correspondence

mteitell@mednet.ucla.edu

In Brief

α-ketoglutarate (αKG) is an important cofactor for demethylation reactions that helps to maintain naive pluripotent stem cells. TeSlaa et al. show that at later stages of pluripotency, αKG can promote early differentiation, highlighting that the cellular context and potentially the stage of cellular maturity can alter the effect of αKG.

TeSlaa et al., 2016, Cell Metabolism *24*, 1–9
September 13, 2016
http://dx.doi.org/10.1016/j.cmet.2016.07.002

CellPress

Please cite this article in press as: TeSlaa et al., α-Ketoglutarate Accelerates the Initial Differentiation of Primed Human Pluripotent Stem Cells, Cell Metabolism (2016), http://dx.doi.org/10.1016/j.cmet.2016.07.002

Cell Metabolism
Short Article

α-Ketoglutarate Accelerates the Initial Differentiation of Primed Human Pluripotent Stem Cells

Tara TeSlaa,[1] Andrea C. Chaikovsky,[2] Inna Lipchina,[3] Sandra L. Escobar,[4] Konrad Hochedlinger,[3] Jing Huang,[1,5,6] Thomas G. Graeber,[5,6,7,8] Daniel Braas,[5,7] and Michael A. Teitell[1,2,6,8,9,10,*]
[1]Molecular Biology Interdepartmental Program, University of California, Los Angeles, Los Angeles, CA 90095, USA
[2]Department of Pathology and Laboratory Medicine, David Geffen School of Medicine, University of California, Los Angeles, Los Angeles, CA 90095, USA
[3]Department of Molecular Biology, Cancer Center and Center for Regenerative Medicine, Massachusetts General Hospital and Harvard Medical School, Boston, MA 02114, USA
[4]Department of Biology, California State University, Northridge, Northridge, CA 91330, USA
[5]Department of Molecular and Medical Pharmacology, Crump Institute for Molecular Imaging, David Geffen School of Medicine, University of California, Los Angeles, Los Angeles, CA 90095, USA
[6]Jonsson Comprehensive Cancer Center, University of California, Los Angeles, Los Angeles, CA 90095, USA
[7]UCLA Metabolomics Center, University of California, Los Angeles, Los Angeles, CA 90095, USA
[8]California NanoSystems Institute, University of California, Los Angeles, Los Angeles, CA 90095, USA
[9]Department of Bioengineering, Department of Pediatrics, and Broad Center for Regenerative Medicine and Stem Cell Research, University of California, Los Angeles, Los Angeles, CA 90095, USA
[10]Lead Contact
*Correspondence: mteitell@mednet.ucla.edu
http://dx.doi.org/10.1016/j.cmet.2016.07.002

SUMMARY

Pluripotent stem cells (PSCs) can self-renew or differentiate from naive or more differentiated, primed, pluripotent states established by specific culture conditions. Increased intracellular α-ketoglutarate (αKG) was shown to favor self-renewal in naive mouse embryonic stem cells (mESCs). The effect of αKG or αKG/succinate levels on differentiation from primed human PSCs (hPSCs) or mouse epiblast stem cells (EpiSCs) remains unknown. We examined primed hPSCs and EpiSCs and show that increased αKG or αKG-to-succinate ratios accelerate, and elevated succinate levels delay, primed PSC differentiation. αKG has been shown to inhibit the mitochondrial ATP synthase and to regulate epigenome-modifying dioxygenase enzymes. Mitochondrial uncoupling did not impede αKG-accelerated primed PSC differentiation. Instead, αKG induced, and succinate impaired, global histone and DNA demethylation in primed PSCs. The data support αKG promotion of self-renewal or differentiation depending on the pluripotent state.

INTRODUCTION

Human pluripotent stem cells (hPSCs) may self-renew or differentiate into all three germ layers (Takahashi et al., 2007; Thomson et al., 1998), but use in regenerative medicine is limited by generally inefficient differentiation strategies (Blanpain et al., 2012). During in vitro differentiation, hPSCs undergo a metabolic shift that increases respiration (oxidative phosphorylation [OXPHOS]) and reduces glycolysis, with inhibition of this transition impeding differentiation (Moussaieff et al., 2015; Zhang et al., 2011; Zhou et al., 2012). Despite the importance of this metabolic shift, differentiation protocols have focused on manipulating key signaling pathways and have overlooked metabolic contributions.

α-ketoglutarate (αKG), a tricarboxylic acid (TCA) cycle metabolite, is a cofactor for αKG-dependent dioxygenase enzymes, which include JmjC-domain containing histone demethylases (JHDMs) and ten-eleven translocation (TET) enzymes (Kaelin and McKnight, 2013). αKG can also bind and block the mitochondrial ATP synthase and inhibit mechanistic target of rapamycin (mTOR) signaling (Chin et al., 2014). Addition of cell-permeable dimethyl-αKG (dm-αKG) to culture media enhances self-renewal and inhibits the differentiation of naive-state mouse embryonic stem cells (mESCs) likely by promoting histone and DNA demethylation (Carey et al., 2015). The hPSCs grown in standard conditions are in a primed, or more developmentally mature, pluripotent state, similar to post-implantation mouse epiblast stem cells (EpiSCs) (Greber et al., 2010; James et al., 2005; Tesar et al., 2007). A role for αKG in primed mouse or hPSCs has not been explored.

Naive and primed pluripotent stem cells (PSCs) show many molecular differences including self-renewing conditions, epigenetic states, and metabolism (Greber et al., 2010; Leitch et al., 2013; Marks et al., 2012; Ware et al., 2014; Zhou et al., 2012). A consensus naive state for hPSCs, however, remains somewhat elusive. Culture conditions that establish naive-like hPSCs yield slightly different transcriptional profiles (Huang et al., 2014). Uncertainty about whether naive hPSCs offer differentiation advantages over traditional primed hPSCs (Pera, 2014)

emphasizes the remaining importance of primed hPSCs as options for potential clinical applications.

Metabolites other than αKG have been shown to play a role in PSC self-renewal and differentiation. Removal of methionine, which provides methyl groups for DNA and histone methylation, potentiates PSC differentiation (Shiraki et al., 2014). Increased acetyl-coenzyme A delays PSC differentiation and histone acetylation and maintains expression of OCT4 (Moussaieff et al., 2015). Oxygen levels can enhance reprogramming to pluripotency or differentiation of hPSCs, depending on environmental context (Mathieu et al., 2014; Xie et al., 2014). The mESCs are dependent on threonine catabolism for histone and DNA methylation (Shyh-Chang et al., 2013; Wang et al., 2009). Here, we investigate the role for αKG during primed PSC differentiation.

RESULTS

TCA Cycle Metabolite Production in hPSCs

Respiration is reduced in hPSCs compared to their differentiated counterparts, suggesting that TCA cycle metabolite production could be low (Zhang et al., 2011; Zhou et al., 2012). To examine the TCA cycle, stable isotope labeling experiments were performed in Essential 8 (E8) media promoting self-renewal or Essential 6 (E6) media encouraging differentiation (Figures S1A and S1B). Using the E8 or E6 system, culture media differ by only two factors that are excluded from the E6 media, basic fibroblast growth factor (bFGF) and transforming growth factor β (TGF-β), ensuring differences in metabolism are due to different cell states. A shift in the oxygen consumption rate (OCR)-to-extracellular acidification rate (ECAR) ratio confirmed a shift toward OXPHOS with E6 media differentiation (Figure 1A). Furthermore, glutamine withdrawal reduced oxygen consumption, implicating glutamine as a TCA cycle fuel in hPSCs (Figure 1B).

Despite a low OCR-to-ECAR ratio, hPSCs showed a robust contribution of [U-^{13}C] glucose into TCA cycle metabolites (Figure 1C). Glutamine withdrawal increased the glucose contribution to TCA cycle metabolites αKG, succinate, and malate in E8, but not in E6, culture conditions (Figure 1C). The mass isotopologue distribution (MID) of citrate indicates the contribution of [U-^{13}C] glucose to the TCA cycle, with m+2 and m+3 isotopologues indicating initial entry of glucose into the TCA cycle and m+4, m+5, and m+6 isotopologues indicating ^{13}C glucose carbons that have cycled through one or two turns (Figure 1D). In glutamine-sufficient conditions, no differences in the citrate MID in E8 and E6 cultures were detected (Figure 1E), but glutamine withdrawal for 18 hr resulted in an increase in m+4 and m+6 citrate isotopologues in undifferentiated human embryonic stem cells (hESCs) (E8) (Figure 1F). Thus, glucose-derived carbons are retained through one or two turns of the TCA cycle in the absence of glutamine in self-renewing hPSCs. Consistent with this result, glutamine withdrawal led to a decrease in unlabeled αKG (m+0) in E8 conditions (Figure S1C).

The MID of citrate with [U-^{13}C] glutamine indicates the amount of citrate derived from glutamine after one turn (m+4) or two turns (m+2) of the TCA cycle (Figure 1G). Increased m+4 citrate was detected in E8 compared to E6 conditions, suggesting a lower contribution of glutamine to the TCA cycle in E6 differentiated hPSCs (Figure 1H). However, 40% of glutamate, which is generated directly from glutamine, was unlabeled in E6 conditions (Figure S1D). Measurement of extracellular glutamate levels revealed net uptake of glutamate by cells cultured in E6 medium (Figure 1I). Detection of [U-^{13}C] glutamate uptake confirmed these results (Figure 1J), with increased conversion of glutamate into αKG occurring in differentiated cells (E6) only in the absence of glutamine (Figure 1K). The data suggest that glucose and glutamine are the major contributors to the TCA cycle in hPSCs; other metabolites, such as glutamate, fuel the TCA cycle in early differentiated hPSCs.

In proliferative cells, αKG-producing transaminases (TAs), which transfer amine groups from glutamate to α-keto acids to form amino acids (Figure S1E), have high activity (Coloff et al., 2016). Glutamine inclusion in hPSC culture medium, which provides glutamate for TAs, increases αKG, alanine, and aspartate levels, products of these TAs (Figures S1F and S1G). To further study TA activity, [$^{15}N_2$] glutamine was used to quantify the transfer of ^{15}N from glutamate to amino acids (Figure S1E), and ^{15}N was detected in alanine, aspartate, isoleucine, serine, and methionine (Figure 1L). Expression of glutamic-pyruvic transaminases (GPTs) and glutamic-oxaloacetic transaminases (GOTs) was confirmed in hPSCs, verifying their contribution to αKG production (Figure S1H). Robust αKG production in primed hPSCs prompted studies into a role for αKG in PSC differentiation.

αKG Accelerates Multi-lineage Primed PSC Differentiation

Neuroectoderm (NE) differentiation was induced in primed H1, H9, UCLA1, and HIPS2 hPSCs by dual SMAD inhibition (Chambers et al., 2009). The dm-αKG significantly increased the percentage of PAX6, an essential transcription factor for NE specification in humans (Zhang et al., 2010), expressing cells by day 4 of differentiation (Figures 2A–2C). MAP2C- and NESTIN-positive cells modestly increased with dm-αKG treatment (Figures 2C and S2A). To determine whether this effect was lineage specific, endoderm differentiation was induced by high-concentration activin A exposure (D'Amour et al., 2005). On day 2, dm-αKG significantly increased the percentage of H9 cells expressing SOX17, a definitive endoderm transcription factor (Figures S2B and S2C). Combined, the data support that αKG accelerates the early differentiation of multiple hPSC germlineages.

NE differentiation was examined with added αKG, which unlike dm-αKG, is dependent on membrane transporters for uptake, and resulted in an increase in PAX6-positive cells (Figures 2D and 2F). In contrast to dm-αKG, which shows a dose-dependent increase in cell differentiation, αKG levels beyond 4 mM did not further stimulate NE differentiation (Figures 2D–2G). Added αKG and dm-αKG each increased intracellular αKG and TCA cycle metabolite levels, although only 12 mM dm-αKG reached significance (Figures 2H and 2I).

Consistent with prior results showing that dm-αKG supports naive mESC self-renewal (Carey et al., 2015), an increase in alkaline phosphatase staining was detected in naive mESCs incubated with dm-αKG during 48 hr of leukemia inhibitory factor (LIF) withdrawal (Figure S2D). Because dm-αKG accelerates primed hPSC differentiation, we examined the role for αKG in primed mouse PSCs, or EpiSCs. Addition of dm-αKG to EpiSCs induced to differentiate by withdrawal of bFGF and activin A

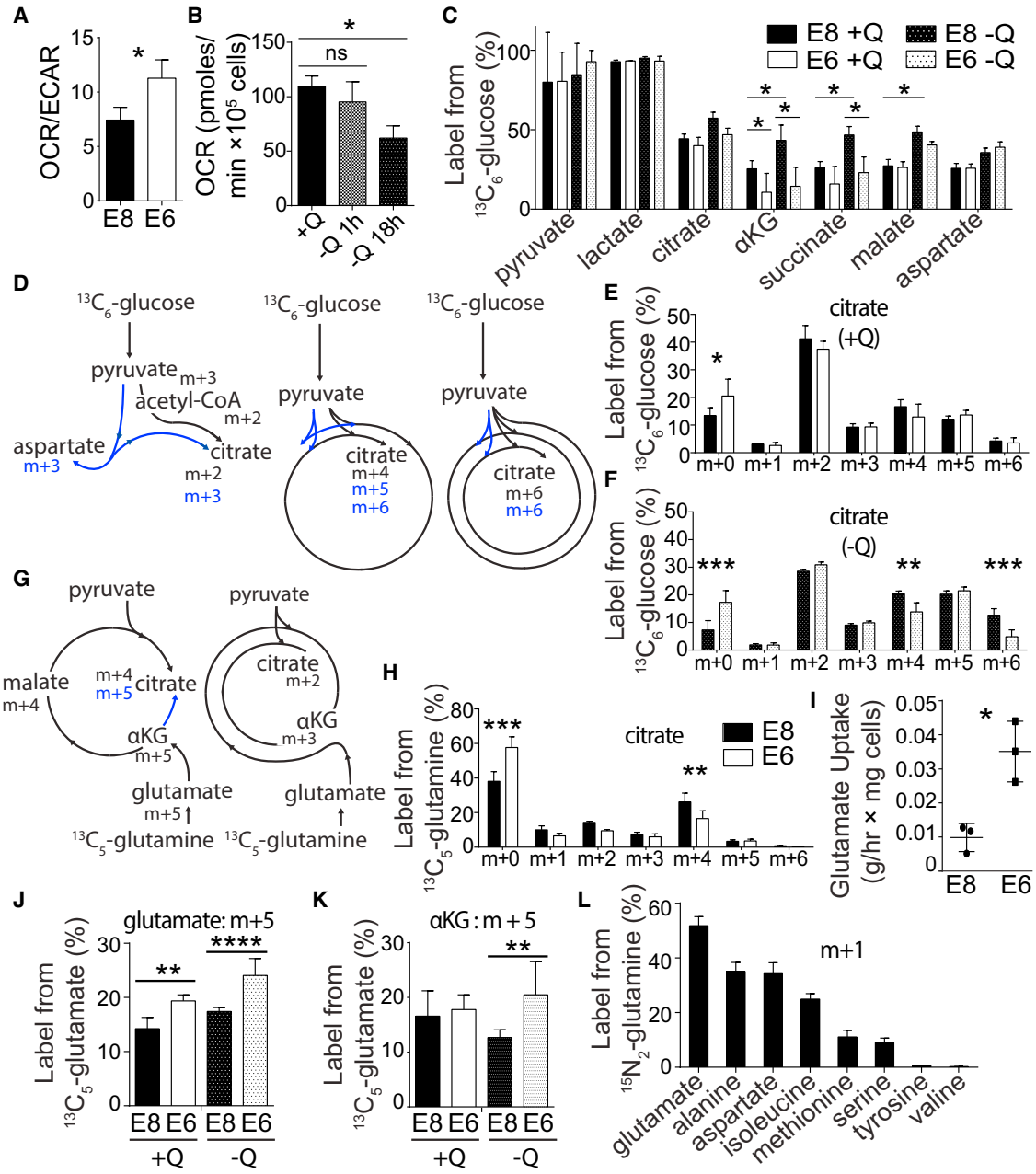

Figure 1. Production of TCA Cycle Metabolites in hPSCs

(A) Ratio of OCR to ECAR in H9 hESCs cultured in medium containing (E8) or lacking (E6) bFGF and TGF-β.

(B) OCR quantified in H9 hESCs grown in media containing glutamine or with glutamine removed for 1 or 18 hr.

(C) Fractional contribution of ^{13}C-labeled metabolites from [U-^{13}C] glucose after 18 hr, quantified by UHPLC-MS.

(D) Schematic illustrating how the MID of citrate from [U-^{13}C] glucose reveals the contribution of glucose-labeled metabolites through multiple turns of the TCA cycle.

(E and F) MID of citrate in H9 hESCs from [U-^{13}C] glucose in conditions containing glutamine (E) or lacking glutamine (F).

(G) Schematic of [U-^{13}C] glutamine labeling of the TCA cycle. The m+5 isotopologue of citrate can be produced by reductive carboxylation of glutamine (blue). The m+4 and m+2 isotopologues contain carbons derived from glutamine after one and two turns of the TCA cycle, respectively.

(H) MID of citrate from [U-^{13}C] glutamine in H9 hESCs cultured in E8 or E6 medium.

(I) Measurement of glutamate uptake from culture medium in H9 hESCs maintained in E8 medium or differentiated in E6 medium.

(J) The m+5 isotopologue of glutamate in H9 hESCs, indicating increased uptake of [U-^{13}C] glutamate from the culture medium in differentiated cells (E6) grown with or without glutamine.

(K) The m+5 isotopologue of αKG in H9 hESCs grown in [U-^{13}C] glutamate.

(L) The m+1 isotopologue of listed amino acids in H9 hESCs grown with [$^{15}N_2$] glutamine, reflecting the activities of multiple αKG-producing TAs.

Data represent mean ± SD of at least three biological replicates. *$p \leq 0.05$; **$p \leq 0.01$; ***$p \leq 0.001$; ****$p \leq 0.0001$. The p values were determined by an unpaired two-tailed Student's t test (A and I) or by one-way ANOVA (B) or two-way ANOVA (C, E, F, H, J, and K) with correction for multiple comparisons.

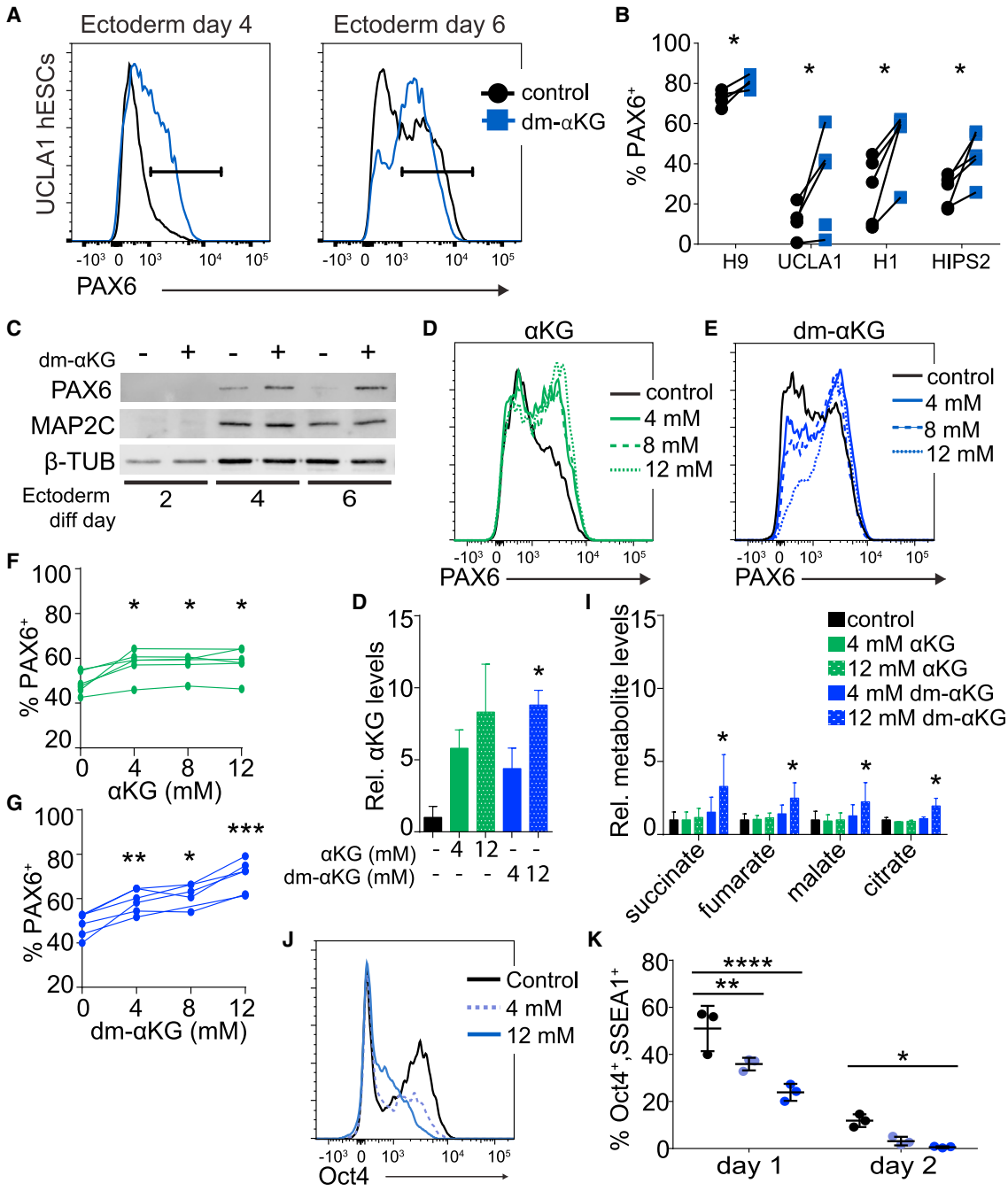

Figure 2. αKG Accelerates Differentiation of Primed PSCs

(A) Flow cytometry analysis of PAX6 transcription factor expression in UCLA1 hESCs encouraged to differentiate into NE at 4 or 6 days. The figure shows 12 mM dm-αKG incubated traces (blue) and control traces (black).

(B) Flow cytometry quantification of the percentage of PAX6-expressing cells at 4 days of NE differentiation for H9, UCLA1, and H1 hESCs and HIPS2 human-induced pluripotent stem cells (hiPSCs). H9, UCLA1, and H1 cells were incubated with (blue) or without (black) 12 mM dm-αKG, and HIPS2 hPSCs were incubated with (blue) or without (black) 6 mM dm-αKG. Lines connect pairs of independent biological replicates.

(C) Immunoblot of ectoderm markers PAX6 and MAP2C after 2, 4, and 6 days of NE differentiation of H9 hESCs.

(D and E) Flow cytometry of PAX6 expression in H9 hESCs on day 4 of NE differentiation, with indicated amounts of αKG (D) or dm-αKG (E) added to the culture medium.

(F and G) Percentage of H9 hESC cells positive for PAX6 expression on day 4 of differentiation plotted against the concentration of added αKG (F) or dm-αKG (G). Lines connect independent biological replicates.

(H and I) UHPLC-MS quantification of fold change of αKG levels (H) and other TCA cycle metabolite levels (I) in H9 hESCs incubated with the listed concentrations of αKG or dm-αKG. Error bars represent SEM of three biological replicates.

(legend continued on next page)

(Greber et al., 2010) accelerated the rate of Oct4 inactivation (Figures 2J, 2K, and S2E–S2G). Therefore, αKG can accelerate differentiation of both mouse and human primed PSCs.

αKG has been shown to bind to and inhibit the mitochondrial ATP synthase subunit β, leading to mTOR inhibition (Chin et al., 2014). To determine whether ATP synthase inhibition contributes to αKG-accelerated primed PSC differentiation, an OXPHOS uncoupling agent, carbonyl cyanide 4-(trifluoromethoxy)-phenylhydrazone (FCCP), was used during NE differentiation. FCCP inhibits ATP production as a mitochondrial inner membrane protonophore that dissipates the H^+ ion electrochemical gradient that runs the ATP synthase. That dm-αKG accelerated NE differentiation in H9 hESCs incubated with FCCP (Figures S2H and S2I) suggested an alternative mechanism. Furthermore, hPSCs treated with an inhibitor of ATP synthase, oligomycin, during NE differentiation showed almost no PAX6 expression after 4 days, despite the addition of pyruvate and uridine to promote cell survival (Figures S2J and S2K) (Birsoy et al., 2015; Sullivan et al., 2015). Because ATP synthase inhibition delays or inhibits NE differentiation, which opposes the accelerating effect of dm-αKG, we conclude that αKG does not accelerate differentiation of primed PSCs through inhibition of ATP synthase.

Succinate Accumulation Delays hPSC Differentiation

A second potential mechanism for αKG-accelerated hPSC differentiation is stimulation of epigenome-modifying dioxygenases. In this event, an αKG-dependent dioxygenase competitive inhibitor, such as succinate (Xiao et al., 2012), would impair differentiation. Cell-permeable succinate, dimethyl succinate (dms), resulted in a decreased percentage of PAX6-expressing hPSCs during NE differentiation compared to hPSCs incubated with dm-αKG alone (Figures S2L and S2M). Inhibition of succinate dehydrogenase A (SDHA), which converts succinate to fumarate either with a chemical inhibitor, 3-nitropropionic acid (NPA), or with small hairpin RNA (shRNA), should also cause succinate accumulation (Figure 3A). NPA treatment decreased the αKG-to-succinate ratio 34-fold, with a 14-fold mean increase in succinate and 2.4-fold mean decrease in αKG (Figures 3B and S3A). NPA delayed NE-specifying PAX6 expression (Figures 3C and S3B–S3D), and the loss of pluripotency marker SSEA3 in hPSCs differentiated into NE (Figure S3E). Knockdown of SDHA, confirmed by immunoblot and reduced OCR (Figures S3F–S3H), also delayed PAX6 and MAP2B expression during NE differentiation, which was rescued by dm-αKG (Figures 3D, 3E, and S3I).

We further assessed the role of succinate in differentiation by embryoid body (EB) formation, which contrasts with lineage-directed differentiation by removal of bFGF rather than by addition of supplements or inhibitors. OCT4 was almost eliminated in EBs expressing a scrambled shRNA, whereas shRNA targeting SDHA maintained elevated OCT4 expression (Figures S3J and S3K). Validating these results, inhibition of SDHA with NPA significantly impaired OCT4 repression in EB differentiation compared to control (Figure S3L).

TA Inhibition Delays hPSC Differentiation

To decrease αKG levels, chemical inhibitors of αKG-producing TAs were used (Figure 3A). Aminooxyacetic acid (AOA), a pan-TA inhibitor, reduced ^{15}N transfer from [$^{15}N_2$] glutamine to alanine, aspartate, isoleucine, serine, and methionine in hPSCs (Figure S3M). L-cycloserine (cyclo), a GPT inhibitor, decreased ^{15}N transfer to alanine in hPSCs treated with cyclo (Figure S3M). Both inhibitors caused a significant decrease in αKG levels and other TCA cycle metabolite levels, but they had no effect on basal respiration (Figures 3F, S3N, and S3O). AOA impaired PAX6 and MAP2B activation during NE differentiation (Figures 3G, 3H, and S3P). A mixture of non-essential amino acids (NEAAs), including alanine and aspartate, had no effect on AOA treatment, whereas supplementation with dm-αKG rescued the block in differentiation caused by AOA (Figures 3G, 3H, and S3P). Cyclo caused a less dramatic, but significant, decrease in the percentage of MAP2B-positive cells, corresponding to its relatively smaller effect on αKG levels compared to AOA (Figures 3I and 3J). Supplementation with dm-αKG restored MAP2B levels in cyclo-treated cells (Figures 3I and 3J). Therefore, decreased αKG levels cause a delay or inhibition of directed differentiation.

To determine whether TCA cycle flux affects differentiation, dichloroacetate (DCA), an inhibitor of pyruvate dehydrogenase kinase (PDK), was used. PDK inhibits pyruvate dehydrogenase (PDH) activity. Therefore, DCA increases PDH activity and glucose flux into the TCA cycle, which elevates electron transport chain (ETC) activity (Figure S4A). Low levels of DCA increased PAX6-positive cells on day 4 of NE differentiation, whereas higher DCA levels had no effect (Figures S4B and S4C). Furthermore, dm-αKG enhanced differentiation at 0 and 3 mM DCA but not at 1 mM (Figures S4B and S4C). These results do not support changes in TCA cycle flux as a mechanism for αKG in accelerated hPSC differentiation. Rather, the data indicate that succinate delays and αKG promotes the initial differentiation of primed PSCs, most likely through actions on αKG-dependent dioxygenases.

αKG/Succinate Regulates the Epigenome of Differentiating hPSCs

To evaluate the role of αKG-dependent dioxygenases during hPSC differentiation, an inhibitory αKG mimetic, dimethyloxalylglycine (dmog) was used. Exposure to dmog inhibited PAX6 expression at concentrations that did not affect cell number (Figures 4A, 4B, and S4D). To assess the effect of the αKG on TET enzymes, dot blots were performed and levels of 5-hydroxymethylcytosine (5hmc) and 5-methylcytosine (5mc) in DNA were measured from H9 and UCLA1 hESCs after 4 days of NE differentiation. Although dm-αKG exposure caused a 2-fold increase in the 5hmc-to-5mc ratio, NPA caused a significant decrease in this ratio (Figures 4C, 4D, and S4E). The data suggest a significant role for TET enzymes in αKG-accelerated differentiation of primed hPSCs. To evaluate αKG regulation of JHDMs, histone

(J and K) Flow cytometry analysis (J) and quantification (K) of Oct4 expression in EpiSC-1 cells differentiated by growth factor withdrawal for 24 hr under control conditions, with 4 mM dm-αKG or with 12 mM dm-αKG.

Data represent mean ± SD of three biological replicates unless otherwise noted. *$p \leq 0.05$; **$p \leq 0.01$; ***$p \leq 0.001$; ****$p \leq 0.0001$. The p values were determined by a ratio-paired two-tailed Student's t test (B, F, G, and H) or by two-way ANOVA with repeated measures and with correction for multiple comparisons (I and K).

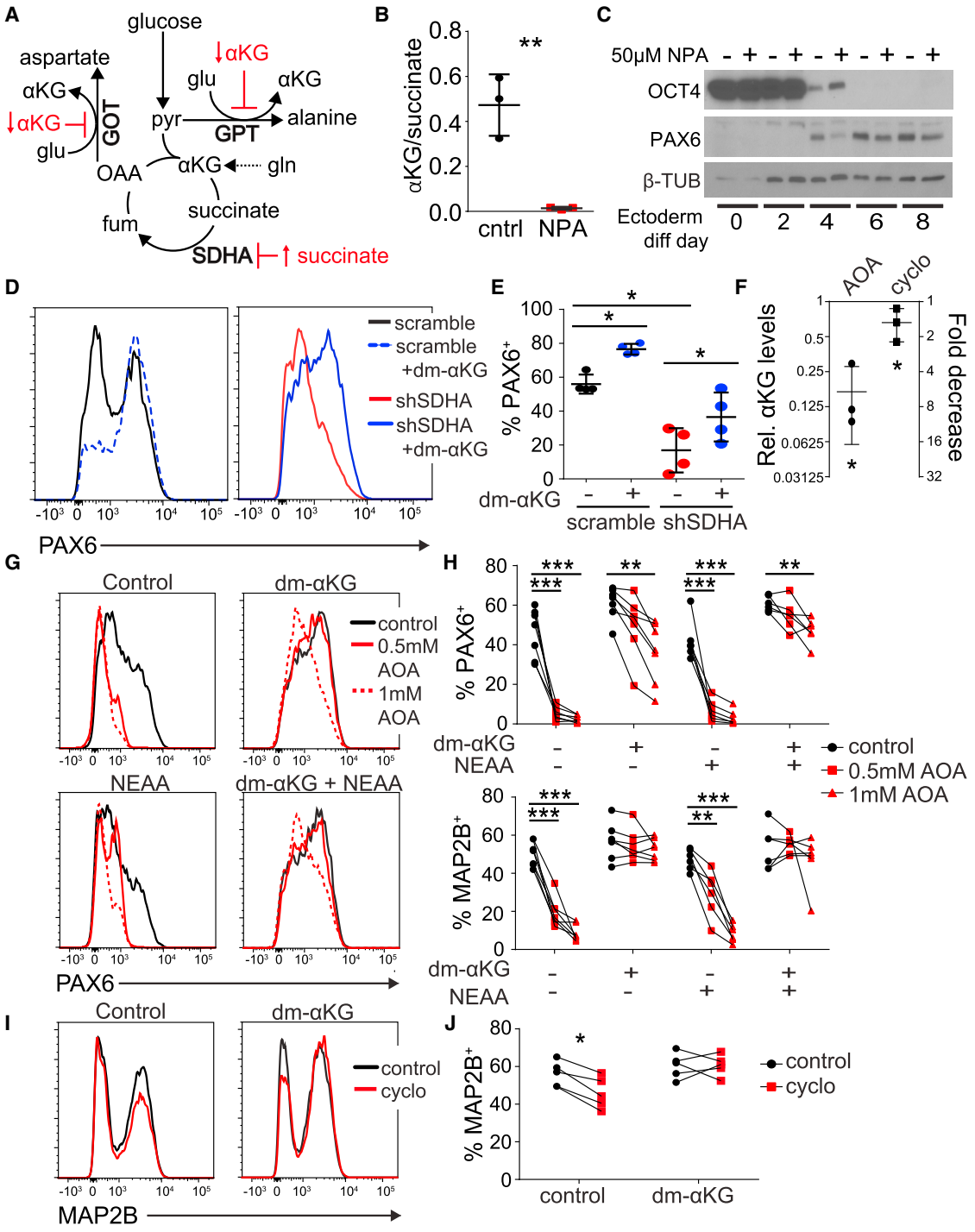

Figure 3. Decrease in the αKG-to-Succinate Ratio Delays hPSC Differentiation

(A) Inhibition or depletion of SDHA causes succinate accumulation. Inhibition of TAs, such as GPT or GOT, results in a decrease in αKG levels. Both of these manipulations cause a decrease in the αKG-to-succinate ratio, which is predicted to inhibit αKG-dependent dioxygenases.

(B) The αKG-to-succinate ratio in control (black) or 10 μM NPA incubated (red) H9 hESCs for 18 hr, quantified by UHPLC-MS.

(C) Immunoblot of OCT4 and PAX6 at indicated time points of NE differentiation with or without 50 μM NPA for H9 hESCs. β-TUB, β-tubulin.

(D and E) Flow cytometry analysis of PAX6 expression in H9 hESCs expressing shRNA targeting SDHA or scramble control shRNA treated with dm-αKG where indicated at day 4 of NE differentiation.

(F) UHPLC-MS quantification of fold change in αKG levels with TA inhibitors AOA and cyclo compared to drug carrier controls.

(legend continued on next page)

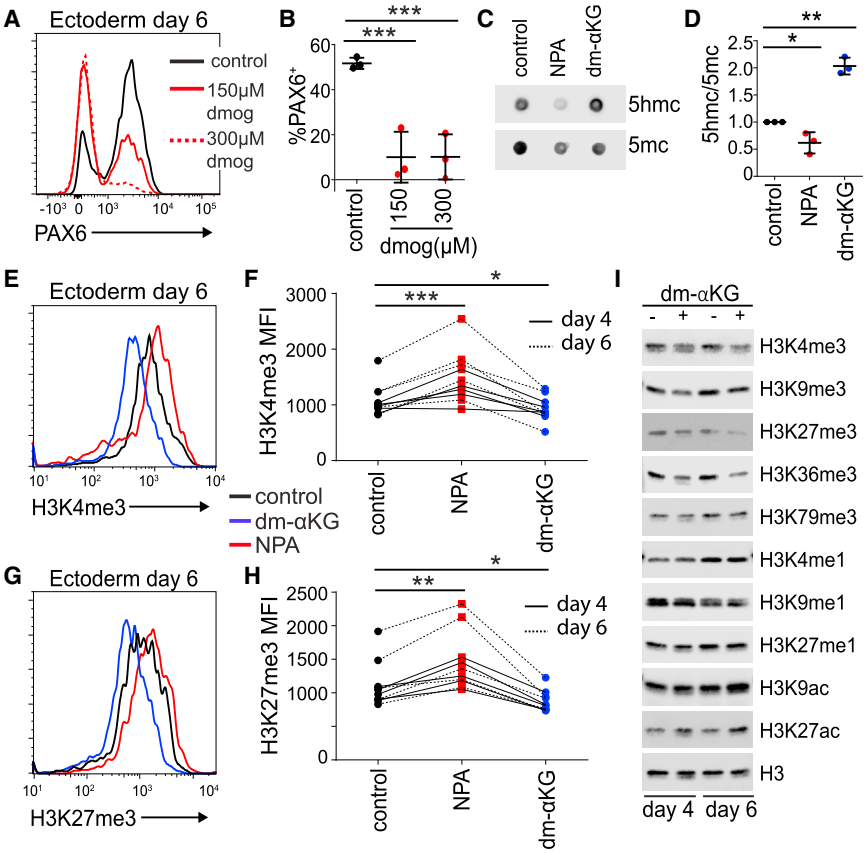

Figure 4. Changes in the α-KG-to-Succinate Ratio Alter DNA Hydroxymethylation and Histone Methylation

(A and B) Flow cytometry analysis of PAX6 expression in H9 hESCs after 6 days of NE differentiation with the indicated concentrations of the αKG-dependent dioxygenase inhibitor, dmog.

(C and D) Dot blot quantification of 5hmc and 5mc in DNA from H9 hESCs after 4 days of NE differentiation under control conditions or with 50 μM NPA or 12 mM dm-αKG added.

(E and F) Flow cytometry analysis of the H3K4me3 mark shown as mean fluorescent intensity (MFI) for UCLA1 hESCs at 4 days (solid line) or 6 days (dotted line) of NE differentiation incubated without (black) or with 12 mM dm-αKG (blue) or 50 μM NPA (red). Lines connect independent biological replicates.

(G and H) Flow cytometry analysis of the H3K27me3 mark shown as MFI for UCLA1 hESCs at 4 days (solid line) or 6 days (dotted line) of NE differentiation incubated without (black) or with 12 mM dm-αKG (blue) or 50 μM NPA (red). Lines connect independent biological replicates.

(I) Immunoblot of histone methylation and acetylation marks in UCLA1 hESCs differentiated into NE at 4 or 6 days with or without dm-αKG incubation.

Data represent mean ± SD of at least three biological replicates. *p ≤ 0.05; **p ≤ 0.01; ***p ≤ 0.001. The p values were determined by one-way ANOVA (B and C) or two-way ANOVA (F and H), with repeated measures and correction for multiple comparisons.

lysine 4 trimethylation (H3K4me3) and histone lysine 27 trimethylation (H3K27me3) were assessed by intracellular flow cytometry. In general, NPA treatment during NE differentiation in UCLA1 hESCs led to an increase in histone marks, whereas dm-αKG led to a decrease (Figures 4E–4H and S4F–S4J). Analysis of an array of histone post-translational modifications by immunoblot revealed an overall repressive effect of dm-αKG on global lysine trimethylation but little effect on global monomethylation or acetylation marks (Figure 4I).

Overall, the data suggest that an increased αKG-to-succinate ratio accelerates, and a decreased αKG-to-succinate ratio retards, initial primed PSC differentiation by titered cofactor/inhibitor activities on epigenome remodeling enzymes, including TET enzymes and JHDMs. This interpretation is consistent with the proposed αKG/succinate mechanism for maintained naive pluripotency in mESCs through epigenetic regulation (Carey et al., 2015), only with an inverse cell fate outcome in the primed pluripotent state with induced differentiation.

DISCUSSION

This study reveals an unanticipated differentiation-promoting role for αKG in primed PSCs. Results have shown that αKG supports self-renewal of naive mESCs, potentially by promoting the demethylation of histones and DNA (Carey et al., 2015). Our data support a similar mechanism with an opposite outcome in the context of primed PSCs induced to differentiate. Consistent with a context-specific role for αKG, TET enzymes and JHDMs have dual roles in the self-renewal and differentiation of mESCs. TET1 promotes reprogramming to naive pluripotency, whereas triple knockout of the TET enzymes impedes differentiation (Costa et al., 2013; Dawlaty et al., 2014). JHDMs are a large class of enzymes that have functions in both naive pluripotency and differentiation. For example, JMJD3 and UTX promote naive pluripotency (Carey et al., 2015), whereas Jarid1b is involved in neural differentiation (Schmitz et al., 2011). The data suggest that αKG enhances the activity of a large family of enzymes that may both maintain low DNA and histone methylation levels, favoring the naive PSC state, and promote epigenome remodeling during induced primed PSC differentiation. These opposing outcomes are consistent with the state-dependent effects of oxygen levels in maintaining pluripotency or promoting differentiation (Mathieu et al., 2014; Xie et al., 2014). Both DNA and histone methylation levels are lower in naive compared to primed PSCs (Hackett and Surani, 2014; Leitch et al., 2013). These epigenome differences, along with metabolome differences

(G–J) Flow cytometry analysis of PAX6 and MAP2B expression in H9 hESCs on day 4 of NE differentiation co-incubated with AOA (G and H) or 50 μM cyclo (I and J) supplemented with 12 mM dm-αKG, 1 mM NEAAs, or both where indicated.

Data represent mean ± SD of at least three biological replicates. *p ≤ 0.05; **p ≤ 0.01; ***p ≤ 0.001. The p values were determined by unpaired Student's t test (B and F) or by one-way ANOVA (E) or two-way ANOVA (H and J) with correction for multiple comparisons.

between naive and primed pluripotent states, could support a differential role for αKG identified in this study. Our results suggest a model for αKG promotion of induced differentiation by primed PSCs from demethylation reactions that help silence pluripotency genes and activate lineage-specific genes to accelerate induced multi-lineage differentiation. A key goal of hPSC research is to develop mature and functional cells for regenerative medicine. Increased αKG could be useful for improving primed-state PSC differentiation.

EXPERIMENTAL PROCEDURES

Standard procedures were followed for immunoblotting, confocal microscopy, and shRNA knockdown, as described in the Supplemental Experimental Procedures. Maintenance of university compliance, including ESCRO, IRB, and Biological Safety, was overseen by K.H. and M.A.T.

Cell Culture

Primed hPSCs were passaged onto feeder-free matrigel (Fisher Scientific) in mTeSR1 medium with Gentle Cell Dissociation Reagent (STEMCELL) for most experiments. For experiments performed in E8 or E6 media (STEMCELL), hPSCs were switched from mTeSR1 to appropriate media at passage. EpiSCs were grown in feeder-free conditions in medium containing bFGF and activin A on fibronectin. Further details are provided in the Supplemental Experimental Procedures.

Seahorse Measurements

OCR and ECAR assays were performed as previously described (Zhang et al., 2012). The hPSCs were plated onto an XF24 microplate (Seahorse Bioscience) at 10^5 or 10^6 cells/well with 10 μM Y-27632 (BioPioneer). The next day, 1 hr before the assay, the medium was changed to XF Media (Seahorse Bioscience) supplemented with 17.5 mM glucose. Cell metabolic rates were measured using an XF24 Extracellular Flux Analyzer (Seahorse Bioscience). Basal respiration was determined by quantifying OCR before and after the addition of 1 μM rotenone and 1 μM antimycin A (Sigma).

Metabolite Extraction and Analysis

Cellular metabolites were extracted with 80% ice-cold methanol, and ultra-high performance liquid chromatography-mass spectrometry (UHPLC-MS) measurements of metabolite levels were performed and analyzed as previously described (Thai et al., 2014). Details are provided in the Supplemental Experimental Procedures.

Glutamate Uptake

Levels of glutamate in culture media were measured using a BioProfile Basic Analyzer (Nova Biomedical). Details are provided in the Supplemental Experimental Procedures.

NE Differentiation

NE differentiation was performed as previously reported (Chambers et al., 2009; Shiraki et al., 2014). Details are provided in the Supplemental Experimental Procedures.

Flow Cytometry Analysis

Cells were collected with Gentle Cell Dissociation Reagent and processed using the Cytofix/Cytoperm Kit (BD Biosciences). Cells were analyzed with either LSRII or LSRFortessa (BD Biosciences).

Dot Blot Analysis and Quantification

DNA was collected with the DNeasy Blood and Tissue Kit (QIAGEN) and quantified using a NanoDrop 1000 spectrophotometer (Thermo Fisher Scientific). DNA was denatured at 99°C for 5 min, put on ice, and neutralized by adding ammonium acetate to a final concentration of 0.66 M. Then, 400 ng of each sample were spotted on Amersham Hybond-N+ (Fisher) nylon membranes and baked at 80°C for 2 hr. Membranes were blocked with 5% skim milk for 3 hr and incubated with primary antibody overnight. The immunoblot procedure was followed. Blots were imaged with an Odyssey Fc and quantified with Image Studio v.5.2.5 (LI-COR Biosciences).

Statistical Analysis

Values are presented as mean ± SD or mean ± SEM. Data were analyzed with Prism (GraphPad). Pairwise comparisons were analyzed using two-tailed Student's t test. Other data were analyzed using one-way or two-way ANOVA with correction for multiple comparisons. In all cases, $p < 0.05$ was considered significant.

SUPPLEMENTAL INFORMATION

Supplemental Information includes Supplemental Experimental Procedures and four figures and can be found with this article online at http://dx.doi.org/10.1016/j.cmet.2016.07.002.

AUTHOR CONTRIBUTIONS

T.T., A.C.C., S.L.E., and D.B. performed experiments. I.L. and K.H. provided key reagents and expert guidance. T.T., J.H., T.G.G., D.B., and M.A.T. participated at differing levels in designing the study and analyzing data. T.T. and M.A.T. wrote the paper with help from T.G.G. and D.B. Maintenance of university compliance, including ESCRO, IRB, and Biological Safety, was overseen by K.H. and M.A.T.

ACKNOWLEDGMENTS

We thank Jinghua Tang for hPSC lines (BSCRC, UCLA), Laurent Vergnes and the UCLA Cellular Bioenergetics Core for technical assistance, Kathrin Plath and Anna Sahakyan for invaluable discussions, and Mahta Nilli, Esther Nuebel, and Kiyoko Miyata for helpful discussions and technical advice. T.T. is supported by a Ruth L. Kirschstein National Research Service award (GM007185) and by the Broad Stem Cell Research Center at UCLA. M.A.T. is supported by the California Institute for Regenerative Medicine (CIRM) (Basic Biology RB1-01397 and Tools & Technologies RT3-07678), UC Discovery/NantWorks Biotechnology (Bio07-10663 and 178517), and NIH (GM073981, P01GM081621, CA156674, CA90571, GM114188, and CA185189). T.G.G. is supported by an American Cancer Society Research Scholar award (RSG-12-257-01-TBE).

Received: July 13, 2015
Revised: February 20, 2016
Accepted: July 1, 2016
Published: July 28, 2016

REFERENCES

Birsoy, K., Wang, T., Chen, W.W., Freinkman, E., Abu-Remaileh, M., and Sabatini, D.M. (2015). An essential role of the mitochondrial electron transport chain in cell proliferation is to enable aspartate synthesis. Cell *162*, 540–551.

Blanpain, C., Daley, G.Q., Hochedlinger, K., Passegué, E., Rossant, J., and Yamanaka, S. (2012). Stem cells assessed. Nat. Rev. Mol. Cell Biol. *13*, 471–476.

Carey, B.W., Finley, L.W.S., Cross, J.R., Allis, C.D., and Thompson, C.B. (2015). Intracellular α-ketoglutarate maintains the pluripotency of embryonic stem cells. Nature *518*, 413–416.

Chambers, S.M., Fasano, C.A., Papapetrou, E.P., Tomishima, M., Sadelain, M., and Studer, L. (2009). Highly efficient neural conversion of human ES and iPS cells by dual inhibition of SMAD signaling. Nat. Biotechnol. *27*, 275–280.

Chin, R.M., Fu, X., Pai, M.Y., Vergnes, L., Hwang, H., Deng, G., Diep, S., Lomenick, B., Meli, V.S., Monsalve, G.C., et al. (2014). The metabolite α-ketoglutarate extends lifespan by inhibiting ATP synthase and TOR. Nature *510*, 397–401.

Coloff, J.L., Murphy, J.P., Braun, C.R., Harris, I.S., Shelton, L.M., Kami, K., Gygi, S.P., Selfors, L.M., and Brugge, J.S. (2016). Differential glutamate metabolism in proliferating and quiescent mammary epithelial cells. Cell Metab. *23*, 867–880.

Costa, Y., Ding, J., Theunissen, T.W., Faiola, F., Hore, T.A., Shliaha, P.V., Fidalgo, M., Saunders, A., Lawrence, M., Dietmann, S., et al. (2013). NANOG-dependent function of TET1 and TET2 in establishment of pluripotency. Nature *495*, 370–374.

D'Amour, K.A., Agulnick, A.D., Eliazer, S., Kelly, O.G., Kroon, E., and Baetge, E.E. (2005). Efficient differentiation of human embryonic stem cells to definitive endoderm. Nat. Biotechnol. *23*, 1534–1541.

Dawlaty, M.M., Breiling, A., Le, T., Barrasa, M.I., Raddatz, G., Gao, Q., Powell, B.E., Cheng, A.W., Faull, K.F., Lyko, F., and Jaenisch, R. (2014). Loss of Tet enzymes compromises proper differentiation of embryonic stem cells. Dev. Cell *29*, 102–111.

Greber, B., Wu, G., Bernemann, C., Joo, J.Y., Han, D.W., Ko, K., Tapia, N., Sabour, D., Sterneckert, J., Tesar, P., and Schöler, H.R. (2010). Conserved and divergent roles of FGF signaling in mouse epiblast stem cells and human embryonic stem cells. Cell Stem Cell *6*, 215–226.

Hackett, J.A., and Surani, M.A. (2014). Regulatory principles of pluripotency: from the ground state up. Cell Stem Cell *15*, 416–430.

Huang, K., Maruyama, T., and Fan, G. (2014). The naive state of human pluripotent stem cells: a synthesis of stem cell and preimplantation embryo transcriptome analyses. Cell Stem Cell *15*, 410–415.

James, D., Levine, A.J., Besser, D., and Hemmati-Brivanlou, A. (2005). TGFbeta/activin/nodal signaling is necessary for the maintenance of pluripotency in human embryonic stem cells. Development *132*, 1273–1282.

Kaelin, W.G., Jr., and McKnight, S.L. (2013). Influence of metabolism on epigenetics and disease. Cell *153*, 56–69.

Leitch, H.G., McEwen, K.R., Turp, A., Encheva, V., Carroll, T., Grabole, N., Mansfield, W., Nashun, B., Knezovich, J.G., Smith, A., et al. (2013). Naive pluripotency is associated with global DNA hypomethylation. Nat. Struct. Mol. Biol. *20*, 311–316.

Marks, H., Kalkan, T., Menafra, R., Denissov, S., Jones, K., Hofemeister, H., Nichols, J., Kranz, A., Stewart, A.F., Smith, A., and Stunnenberg, H.G. (2012). The transcriptional and epigenomic foundations of ground state pluripotency. Cell *149*, 590–604.

Mathieu, J., Zhou, W., Xing, Y., Sperber, H., Ferreccio, A., Agoston, Z., Kuppusamy, K.T., Moon, R.T., and Ruohola-Baker, H. (2014). Hypoxia-inducible factors have distinct and stage-specific roles during reprogramming of human cells to pluripotency. Cell Stem Cell *14*, 592–605.

Moussaieff, A., Rouleau, M., Kitsberg, D., Cohen, M., Levy, G., Barasch, D., Nemirovski, A., Shen-Orr, S., Laevsky, I., Amit, M., et al. (2015). Glycolysis-mediated changes in acetyl-CoA and histone acetylation control the early differentiation of embryonic stem cells. Cell Metab. *21*, 392–402.

Pera, M.F. (2014). In search of naivety. Cell Stem Cell *15*, 543–545.

Schmitz, S.U., Albert, M., Malatesta, M., Morey, L., Johansen, J.V., Bak, M., Tommerup, N., Abarrategui, I., and Helin, K. (2011). Jarid1b targets genes regulating development and is involved in neural differentiation. EMBO J. *30*, 4586–4600.

Shiraki, N., Shiraki, Y., Tsuyama, T., Obata, F., Miura, M., Nagae, G., Aburatani, H., Kume, K., Endo, F., and Kume, S. (2014). Methionine metabolism regulates maintenance and differentiation of human pluripotent stem cells. Cell Metab. *19*, 780–794.

Shyh-Chang, N., Locasale, J.W., Lyssiotis, C.A., Zheng, Y., Teo, R.Y., Ratanasirintrawoot, S., Zhang, J., Onder, T., Unternaehrer, J.J., Zhu, H., et al. (2013). Influence of threonine metabolism on S-adenosylmethionine and histone methylation. Science *339*, 222–226.

Sullivan, L.B., Gui, D.Y., Hosios, A.M., Bush, L.N., Freinkman, E., and Vander Heiden, M.G. (2015). Supporting aspartate biosynthesis is an essential function of respiration in proliferating cells. Cell *162*, 552–563.

Takahashi, K., Tanabe, K., Ohnuki, M., Narita, M., Ichisaka, T., Tomoda, K., and Yamanaka, S. (2007). Induction of pluripotent stem cells from adult human fibroblasts by defined factors. Cell *131*, 861–872.

Tesar, P.J., Chenoweth, J.G., Brook, F.A., Davies, T.J., Evans, E.P., Mack, D.L., Gardner, R.L., and McKay, R.D.G. (2007). New cell lines from mouse epiblast share defining features with human embryonic stem cells. Nature *448*, 196–199.

Thai, M., Graham, N.A., Braas, D., Nehil, M., Komisopoulou, E., Kurdistani, S.K., McCormick, F., Graeber, T.G., and Christofk, H.R. (2014). Adenovirus E4ORF1-induced MYC activation promotes host cell anabolic glucose metabolism and virus replication. Cell Metab. *19*, 694–701.

Thomson, J.A., Itskovitz-Eldor, J., Shapiro, S.S., Waknitz, M.A., Swiergiel, J.J., Marshall, V.S., and Jones, J.M. (1998). Embryonic stem cell lines derived from human blastocysts. Science *282*, 1145–1147.

Wang, J., Alexander, P., Wu, L., Hammer, R., Cleaver, O., and McKnight, S.L. (2009). Dependence of mouse embryonic stem cells on threonine catabolism. Science *325*, 435–439.

Ware, C.B., Nelson, A.M., Mecham, B., Hesson, J., Zhou, W., Jonlin, E.C., Jimenez-Caliani, A.J., Deng, X., Cavanaugh, C., Cook, S., et al. (2014). Derivation of naive human embryonic stem cells. Proc. Natl. Acad. Sci. USA *111*, 4484–4489.

Xiao, M., Yang, H., Xu, W., Ma, S., Lin, H., Zhu, H., Liu, L., Liu, Y., Yang, C., Xu, Y., et al. (2012). Inhibition of α-KG-dependent histone and DNA demethylases by fumarate and succinate that are accumulated in mutations of FH and SDH tumor suppressors. Genes Dev. *26*, 1326–1338.

Xie, Y., Zhang, J., Lin, Y., Gaeta, X., Meng, X., Wisidagama, D.R., Cinkornpumin, J., Koehler, C.M., Malone, C.S., Teitell, M.A., and Lowry, W.E. (2014). Defining the role of oxygen tension in human neural progenitor fate. Stem Cell Reports *3*, 743–757.

Zhang, J., Khvorostov, I., Hong, J.S., Oktay, Y., Vergnes, L., Nuebel, E., Wahjudi, P.N., Setoguchi, K., Wang, G., Do, A., et al. (2011). UCP2 regulates energy metabolism and differentiation potential of human pluripotent stem cells. EMBO J. *30*, 4860–4873.

Zhang, J., Nuebel, E., Wisidagama, D.R.R., Setoguchi, K., Hong, J.S., Van Horn, C.M., Imam, S.S., Vergnes, L., Malone, C.S., Koehler, C.M., and Teitell, M.A. (2012). Measuring energy metabolism in cultured cells, including human pluripotent stem cells and differentiated cells. Nat. Protoc. *7*, 1068–1085.

Zhang, X., Huang, C.T., Chen, J., Pankratz, M.T., Xi, J., Li, J., Yang, Y., Lavaute, T.M., Li, X.-J., Ayala, M., et al. (2010). Pax6 is a human neuroectoderm cell fate determinant. Cell Stem Cell *7*, 90–100.

Zhou, W., Choi, M., Margineantu, D., Margaretha, L., Hesson, J., Cavanaugh, C., Blau, C.A., Horwitz, M.S., Hockenbery, D., Ware, C., and Ruohola-Baker, H. (2012). HIF1α induced switch from bivalent to exclusively glycolytic metabolism during ESC-to-EpiSC/hESC transition. EMBO J. *31*, 2103–2116.